Supplement of Clim. Past, 22, 1655–1674, 2026
https://doi.org/10.5194/cp-22-1655-2026-supplement

Climate of the Past
Open Access

Supplement of

Quantifying Southern Hemisphere dust sources during the Last Glacial-Interglacial Transition using rare earth elements in the EPICA Dome C ice core

Sibylle Boxho et al.

Correspondence to: Sibylle Boxho (sibylle.boxho@ulb.be) and Steeve Bonneville (steeve.bonneville@ulb.be)

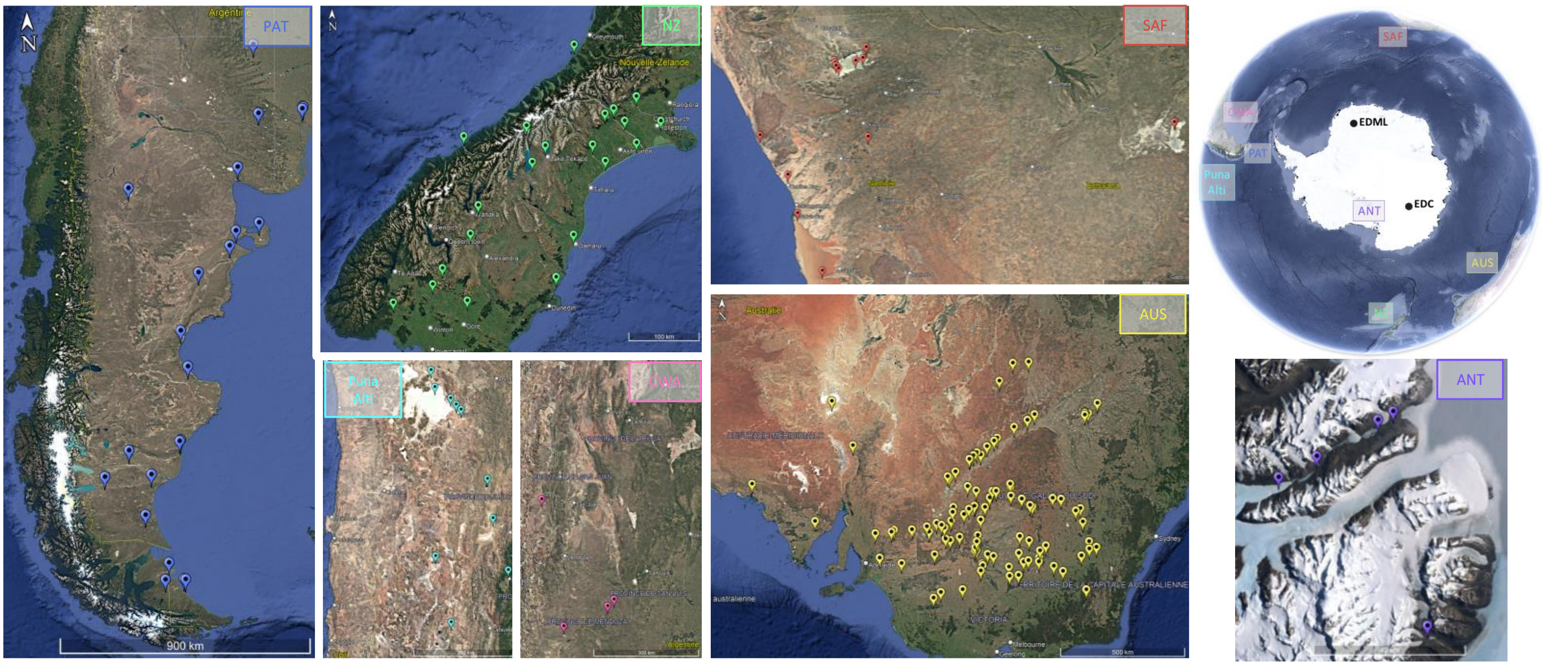
PAT
900 km
NZ
Nouvelle-Zélande
SAF
Puna
Alti
CWA
AUS
Australie
VICTORIA
EDML
EDC
ANT

Figure S1: Location of dust sources (DS) used in our DEEPOT algorithm in Southern South America (including Patagonia, Central Western Argentina and Puna-Altiplano), Southern Africa, South-Eastern Australia, South-Island in New Zealand and Antarctica – McMurdo regions (see Table S1 for details), © Google Earth Pro**.**

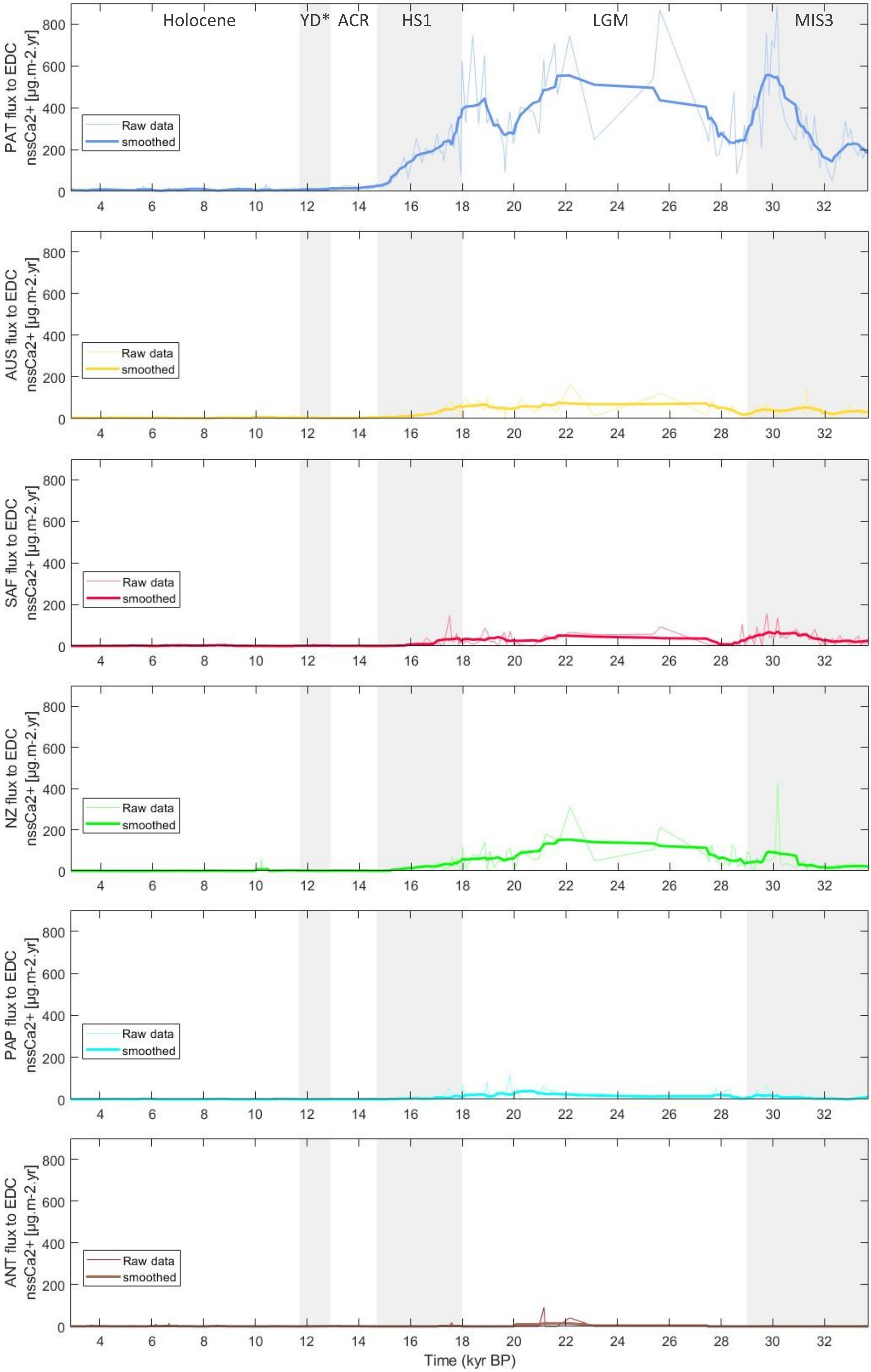

Holocene
YD*
ACR
HS1
LGM
MIS3
PAT flux to EDC nssCa2+ [µg.m-2.yr]
AUS flux to EDC nssCa2+ [µg.m-2.yr]
SAF flux to EDC nssCa2+ [µg.m-2.yr]
NZ flux to EDC nssCa2+ [µg.m-2.yr]
PAP flux to EDC nssCa2+ [µg.m-2.yr]
ANT flux to EDC nssCa2+ [µg.m-2.yr]
Raw data
smoothed
Time (kyr BP)

Figure S2: Reconstruction of the evolution of dust fluxes [contribution (Table S2) * $nssCa^{2+}$ in $\mu g.m^{-2}.yr^{1}$ (Fischer *et al.*, 2007)] from each PSA (PAT, AUS, SAF, PAP, and ANT) to EDC between 2.852 to 33.699 kyr BP. Bold lines denote the mobile average over 9 steps. Gray vertical zones delineate the various periods of the transition from end of MIS3 to Holocene.

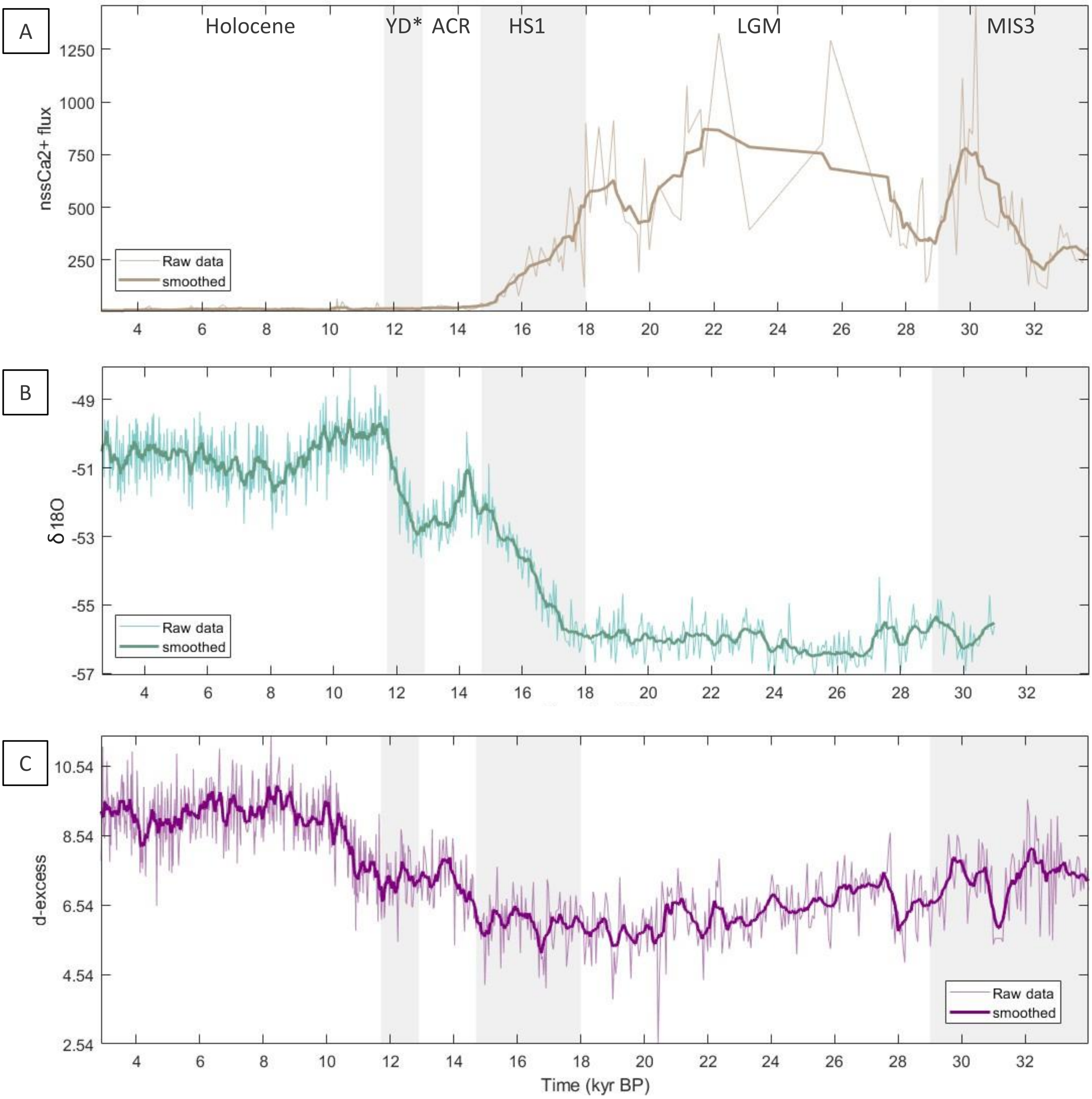
A
Holocene
YD*
ACR
HS1
LGM
MIS3
nssCa2+ flux
Raw data
smoothed
B
δ 18O
Raw data
smoothed
C
d-excess
Raw data
smoothed
Time (kyr BP)

Figure S3: Comparison between 2.852 to 33.699 kyr BP of: (A) Non Sea Salt Calcium ($nssCa^{2+}$) flux in EDC ice core in $\mu g.m^{-2}.yr^{1}$ (Fischer *et al*., 2007); (B) $\delta^{18}O$ in EDC ice core (EPICA Community Members, 2006); and (C) deuterium excess (d-excess) in EDC ice core (Stenni *et al.*, 2010). Bold lines denote the mobile average over 9 steps. Gray vertical zones delineate the various periods of the transition from end of MIS3 to Holocene.

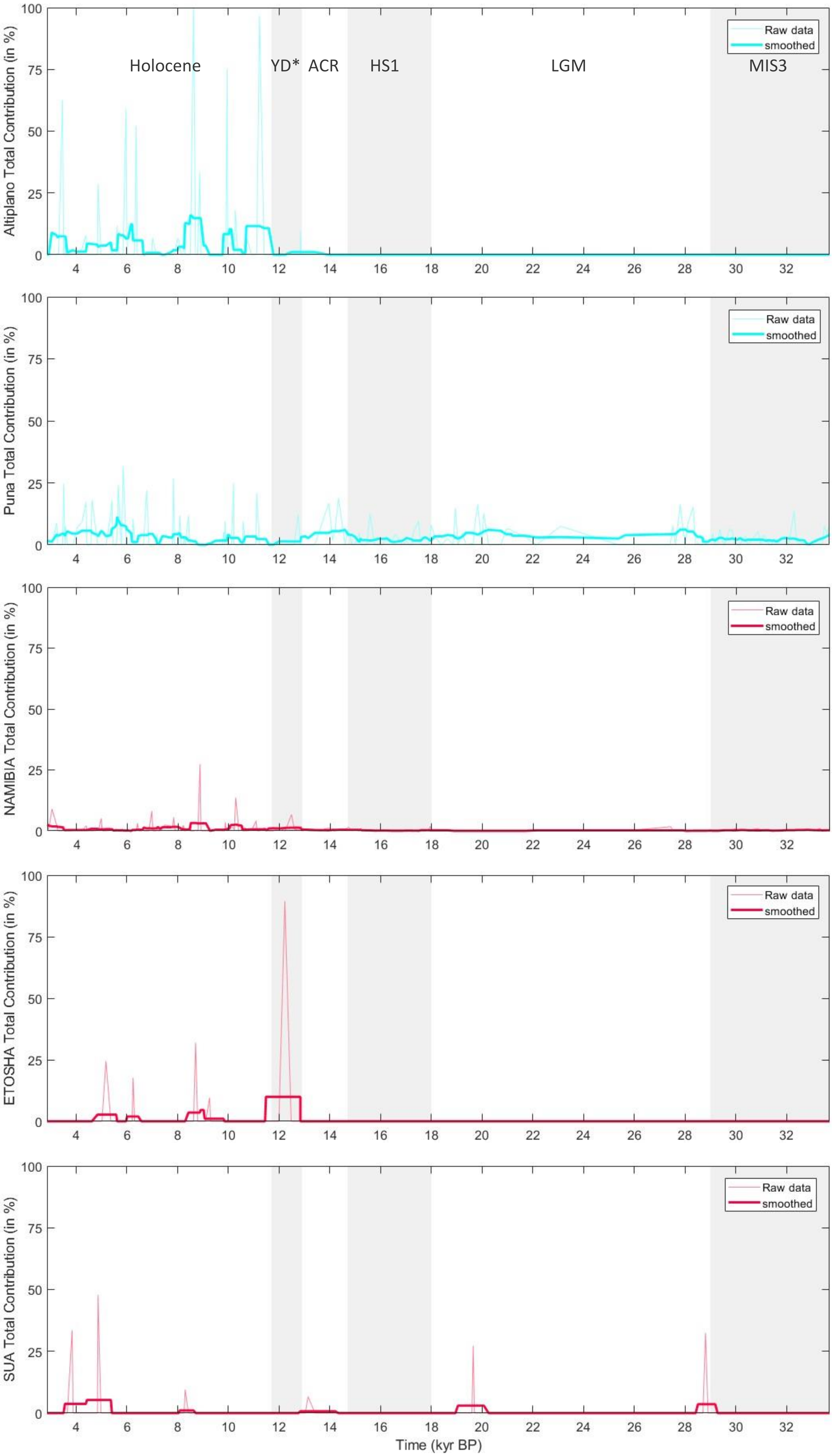

Holocene
YD*
ACR
HS1
LGM
MIS3
Raw data
smoothed
Altiplano Total Contribution (in %)
Puna Total Contribution (in %)
NAMIBIA Total Contribution (in %)
ETOSHA Total Contribution (in %)
SUA Total Contribution (in %)
Time (kyr BP)

Figure S4: Evolution of contribution to EDC from subregions of the Puna-Altiplano and Southern Africa PSA between 2.852 to 33.699 kyr BP (% of total dust deposition for each PSA). Bold lines denote the mobile average over 9 steps. Gray vertical zones delineate the various periods of the transition from end of MIS3 to Holocene.

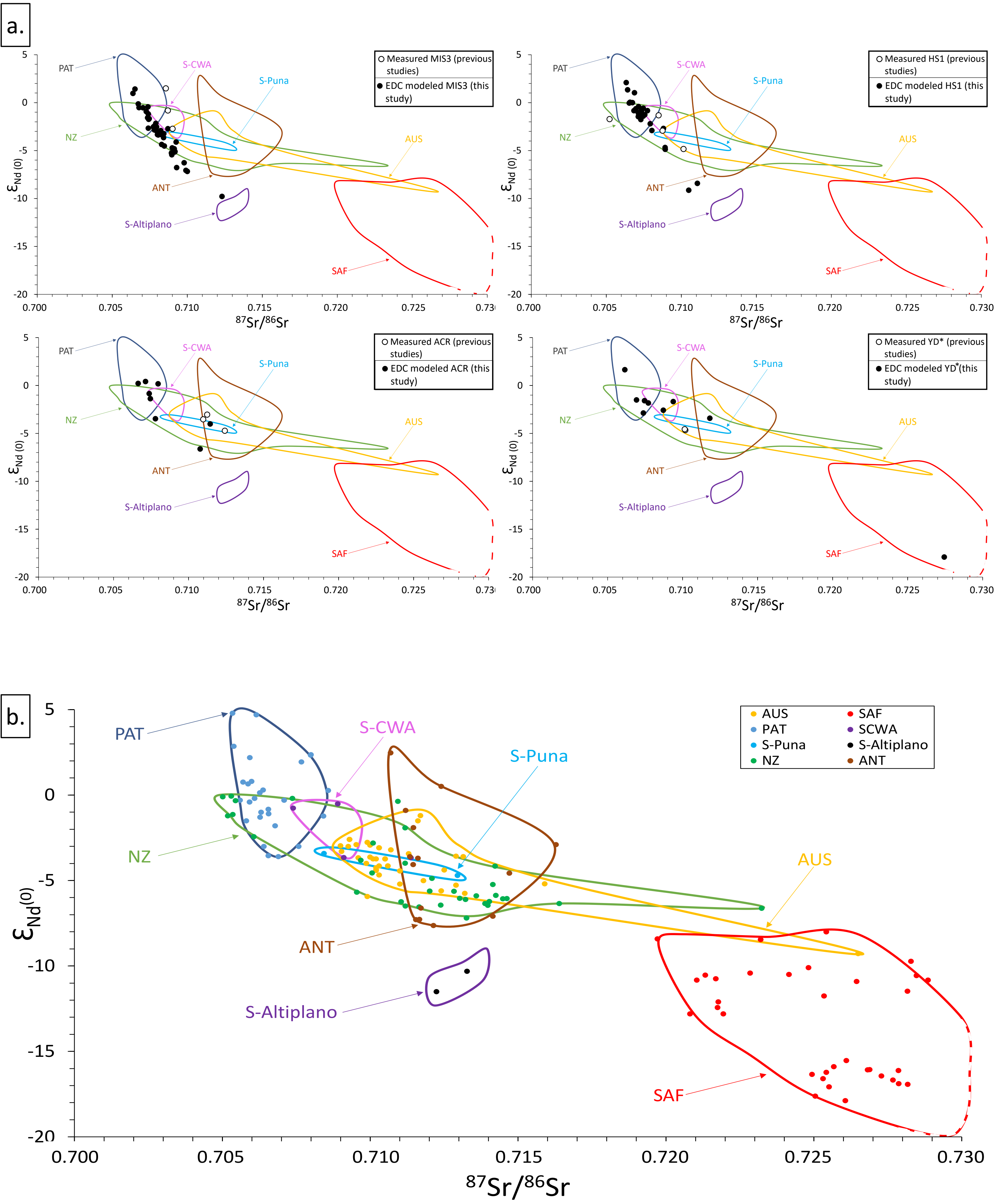

a.
PAT
S-CWA
S-Puna
NZ
AUS
ANT
S-Altiplano
SAF
Measured MIS3 (previous studies)
EDC modeled MIS3 (this study)
Measured HS1 (previous studies)
EDC modeled HS1 (this study)
Measured ACR (previous studies)
EDC modeled ACR (this study)
Measured YD* (previous studies)
EDC modeled YD*(this study)
ε_{Nd} (0)
$^{87}Sr/^{86}Sr$
5
0
-5
-10
-15
-20
0.700
0.705
0.710
0.715
0.720
0.725
0.730
b.
AUS
PAT
S-Puna
NZ
SAF
SCWA
S-Altiplano
ANT
$\varepsilon_{Nd}(0)$
$^{87}Sr/^{86}Sr$

Figure S5*:* (a) Comparison between REE-based modelled $^{87}Sr/^{86}Sr$ and ε_{Nd} values and measured dust isotopic compositions from East Antarctica during the MIS3, HS1, ACR, and YD*, shown together with the isotopic domains of the PSA in the Southern Hemisphere. Measured data (open symbols; references, values, and locations in Table S5; see Figure 2 for other time periods) were obtained from ice cores Taylor Dome (MIS3, HS1, ACR), Old Dome C (HS1), and Taylor Glacier (HS1, ACR, YD*). Modelled expected isotopic compositions (solid symbols; see Section 4.1) were calculated using (i) the contributions of PSA (Table S2) and (ii) the isotopic fingerprints and elemental concentrations of PSA end-members (Table S4). Colored frames delineate the isotopic ranges of the respective PSA sources contributing to the dust assemblage (data from Grousset *et al.*, 1992; Delmonte *et al.*, 2004; Gingele and De Deckker, 2005; De Deckker et al., 2014; Revel-Rolland et al., 2006; Gaiero, 2007; Gili et al., 2017, 2022; Li *et al.*, 2020; Koffman *et al.*, 2021; Blakowski *et al.*, 2014—Table S4). Note that the SAF domain extends beyond the range shown in the figure. (b) Sr-Nd isotope composition data used to construct the isotopic fields for each PSA.

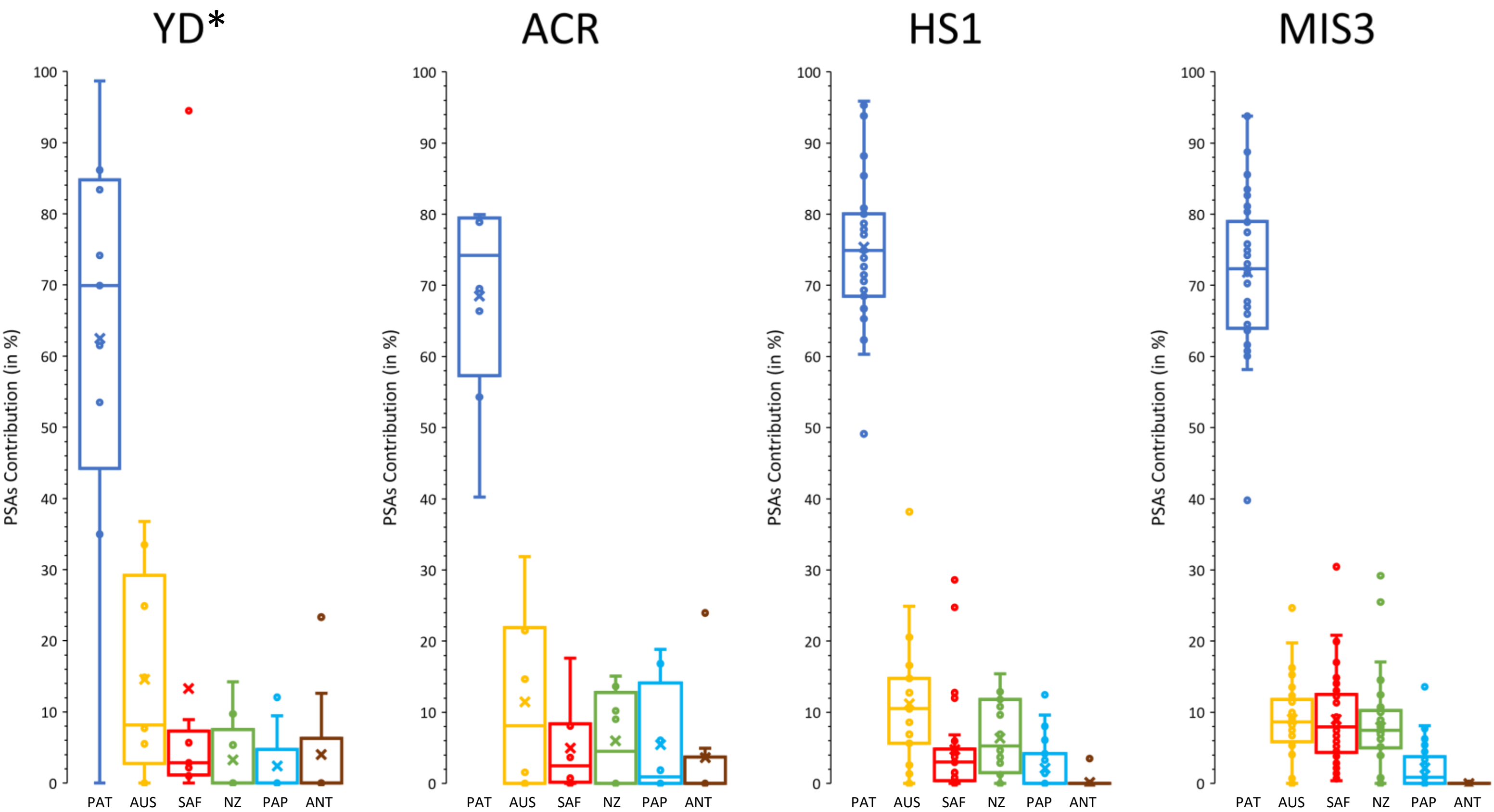
YD*
ACR
HS1
MIS3
PSAs Contribution (in %)
PAT
AUS
SAF
NZ
PAP
ANT

Figure S6: Box plots of main provenance contributions of Younger Dryas (YD*), Antarctica Cold Reveal (ACR), Heindrich Stadial 1 (HS1), and Marine Isotope Stage 3 (MIS3) dust in EDC ice core. Horizontal lines in the boxes indicate the median values of contribution for each source, cross symbols denote the mean and the extremes of the colored boxes indicate the first and third quartiles, and the whiskers indicate the lower and upper extremes.

ADDITIONAL REFERENCES

Aarons, S. M., Aciego, S. M., Gabrielli, P., Delmonte, B., Koornneef, J. M., Wegner, A., and Blakowski, M. A.: The impact of glacier retreat from the Ross Sea on local climate: Characterization of mineral dust in the Taylor Dome ice core, East Antarctica, Earth Planet. Sc. Lett., 444, 34–44, https://doi.org/10.1016/j.epsl.2016.03.035, 2016.

Aarons, S. M., Aciego, S. M., Arendt, C. A., Blakowski, M. A., Steigmeyer, A., Gabrielli, P., Sierra-Hernández, M. R., Beaudon, E., Delmonte, B., Baccolo, G., May, N. W., and Pratt, K. A.: Dust composition changes from Taylor Glacier (East Antarctica) during the last glacial-interglacial transition: A multi-proxy approach, Quaternary Sci. Rev., 162, 60–71, https://doi.org/10.1016/j.quascirev.2017.03.011, 2017.

Delmonte, B., Baroni, C., Andersson, P. S., Schoberg, H., Hansson, M., Aciego, S., Petit, J., Albani, S., Mazzola, C., Maggi, V., and Frezzotti, M.: Aeolian dust in the Talos Dome ice core (East Antarctica, Pacific/Ross Sea sector): Victoria Land versus remote sources over the last two climate cycles, J. Quaternary Sci., 25, 1327–1337, https://doi.org/10.1002/jqs.1418, 2010b

Marx, S. K., Kamber, B. S., and McGowan, H. A.: Provenance of long-travelled dust determined with ultra-trace-element composition: a pilot study with samples from New Zealand glaciers, Earth Surf. Proc. Land., 30, 699–716, https://doi.org/10.1002/esp.1169, 2005

McGowan, H. A., Kamber, B., McTainsh, G. H., and Marx, S. K.: High resolution provenancing of long travelled dust deposited on the Southern Alps, New Zealand, Geomorphology, 69, 208–221, https://doi.org/10.1016/j.geomorph.2005.01.005, 2005.